LABORATORY SIMULATION OF DIRECT LIGHTNING STROKES TO A MODELLED BUILDING – MEASUREMENT OF MAGNETIC FIELDS AND INDUCED VOLTAGES

W. J. Zischank
wolfgang.zischank@unibw-muenchen.de
University of the Federal Armed Forces Munich
Germany

I. A. Metwally
metwally@mans.edu.eg
University of the Federal Armed Forces Munich
Germany

F. Heidler
fridolin.heidler@unibw-muenchen.de
University of the Federal Armed Forces Munich
Germany

J. Wiesinger
gabriele.blochum@unibw-muenchen.de
Puchheim
Germany

A. Kern
a.kern@fh-aachen.de
University of Applied Sciences Aachen
Germany

M. Seevers
MSeevers@HEW.de
Hamburgische Electricitäts-Werke AG
Germany

Abstract: In IEC 61312-2 equations for the assessment of the magnetic fields inside structures due to a direct lightning strike are given. These equations are based on computer simulations for shields consisting of a single-layer steel grid of a given mesh width. Real constructions, however, contain at least two layers of reinforcement steel grids.

The objective of this study was to experimentally determine the additional shielding effectiveness of a second reinforcement layer compared to a single-layer grid. To this end, simulated structures were set up in the high current laboratory. The structures consisted of cubic cages of 2 m side length with one or with two reinforcement grids, respectively. The structures were exposed to direct lightning currents representing the variety of anticipated lightning current waveforms. The magnetic fields and their derivatives at several positions inside the structure as well as the voltage between "floor" and "roof" in the center were determined for different current injection points. From these data the improvement of the shielding caused by a second reinforcement layer is derived.

Keywords: Lightning, electromagnetic shielding, magnetic field, reinforced concrete, induced voltage.

1. INTRODUCTION

Lightning constitutes a severe threat to sensitive electrical or electronic equipment located inside a structure. Due to the ever increasing use and sensitivity of microelectronic circuits and due to the interconnection of equipment by extended information technology networks during the last few decades, the control of the electromagnetic interferences has become the dominant task of lightning protection. As the basic philosophy to control lightning generated electromagnetic interferences, the principle of "Lightning Protection Zones (LPZ)" has been developed by the committee IEC TC 81 and has been laid down in the international standard series IEC 61312 [1, 2]. This principle requires to form nested zones of successively reduced electromagnetic environment. This objective is mainly achieved by two measures:

- shielding to reduce the electromagnetic fields
- equipotential bonding of all lines at the LPZ-boundaries to limit the line conducted overvoltages and currents (e.g. by means of surge protective devices).

A cost effective method to form electromagnetic shields is to use existing metallic structural components, like the reinforcement of concrete. Such structural shields, of course, are leaky shields and therefore it is necessary to know about their effectiveness in reducing the electromagnetic environment.

Most of the previous work in determining electromagnetic fields inside structures has been done for "classical" lightning protection systems (LPS) with distances between the individual (down) conductors in the 10 m range by applying different computational algorithms. Theoretical computation of magnetic fields inside steel structures formed by gridlike spatial shields with mesh

width in the range of a few 10 cm has been presented in [3, 4]. Time-domain analysis of magnetic field inside carbon fiber composite enclosures is shown in [5]. Few experimental work has been done, e.g. [6].

In IEC 61312-2 [2] equations for the assessment of the magnetic fields inside gridlike spatial shields are given as a function of mesh width and location inside the structure. These equations do not exactly represent the field inside for a given configuration. Moreover, they are enveloping curves derived from the computation [3, 4] of numerous configurations of buildings or structures consisting of a single-layer metallic grid.

Real reinforced concrete constructions, however, contain at least two layers of reinforcement steel grids. Therefore, it is desirable to know about the additional shielding effectiveness of a second reinforcement layer in concrete constructions.

In order to determine the improvement of the shielding by a second steel grid layer in reinforced concrete, simulated structures have been set up in the High Current Laboratory of the University of the Federal Armed Forces in Munich (UAFM). The simulated structures consisted of cubic cages of dimensions 2m x 2m x 2m built by reinforcement steel grids. The floor (ground) side was formed by a steel plate. Three configurations (AI, AII, and AIII) of the cage were set up:

- **AI**: Single layer steel grid
- **AII**: Double layer steel grid, inner and outer cage connected only at the four corners of the "roof"
- **AIII**: Double layer steel grid, inner and outer cage connected in a pitch of 50 cm.

Inside these three configurations the magnetic fields and their derivatives were measured in the three coordinates (*x, y, z*) at four positions: in the center of the cage, halfway between center and a wall, close to a wall, and close to a corner. Further the open circuit voltage appearing in the center between the roof and the floor was measured.

The tests were conducted with three impulse current waveforms to cover the whole range of the anticipated lightning current waveforms. The currents of these return strokes are classified according to their front times into: (1) slow waveform with a 10 µs front time representing positive strokes, (2) microsecond waveform with a 1µs front time representing negative first strokes and (3) submicrosecond waveform with a 0,25 µs front time representing negative subsequent strokes.

The test currents were injected into the roof of the outer cage at three different positions: to the center, to middle of a lateral edge, and to the corner. The variations of the cage configuration, test currents, injection points and measured quantities resulted in a data set of more than 350 individual signals.

2. EXPERIMENTAL SETUP

2.1 Test Structure

It is well known that the concrete itself does not significantly contribute to the electromagnetic shielding. Therefore, the test structure is built only of the single- or double-layer steel reinforcement in form of cubic cages. The single layer cage has the dimensions of 2 m x 2 m x 2 m. The sides and the roof of the cages consist of a welded steel rebar grid made of steel rods having a diameter of 6 mm and forming square meshes of 15 cm × 15 cm. A steel square tube (2 cm × 2 cm) is used as a supporting frame at the cage edges. The floor of the cage is made of a 1 mm steel plate to simulate the highly conductive ground. This floor is equipped with a 0,75 m × 1 m access door. All rods of the meshes are welded to the supporting frame and to the floor plate. In the case of the double-layer cage, an inner cage (1,7 m × 1,85 m × 1,7 m) is inserted into the cage described above. The inner cage consists of the same steel reinforcement grid type with the same mesh size. The interspacing between the two cages is kept at 0,15 m. The inner cage, too, is

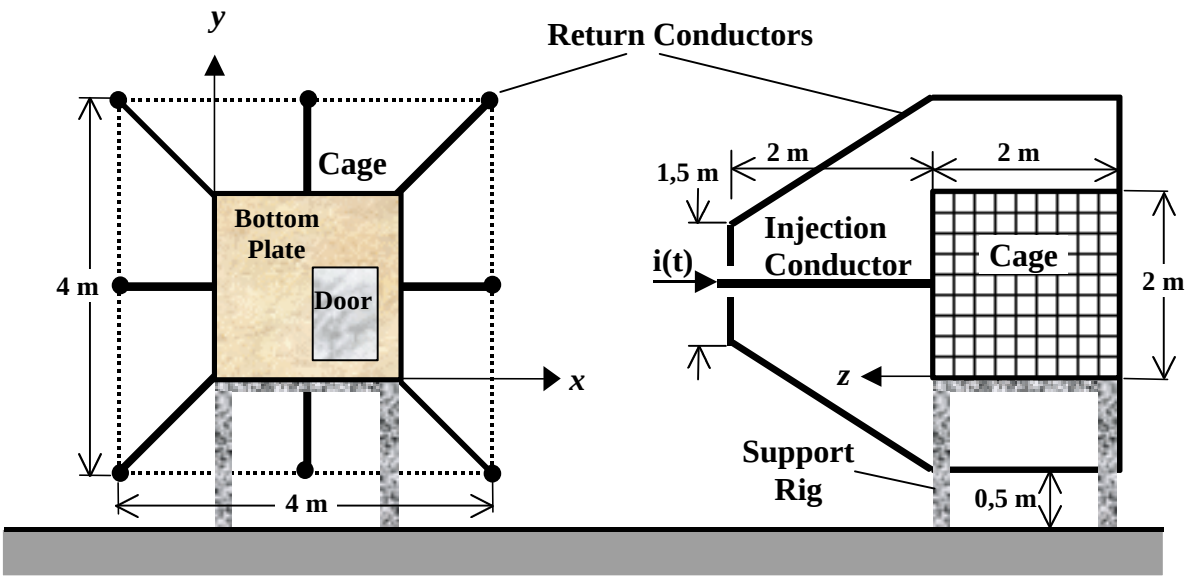

Fig. 1. Arrangement of the cage on the test rig

directly welded to the floor steel plate. The cages are placed on a wooden support rig, 1,5 m above the laboratory floor. The whole test object is rotated 90° (i.e. the roof is pointing to the left and the floor to the right) to facilitate a symmetric arrangement of the structure with respect to the test current generator. Figure 1 illustrates the arrangement of the test structure on the test rig.

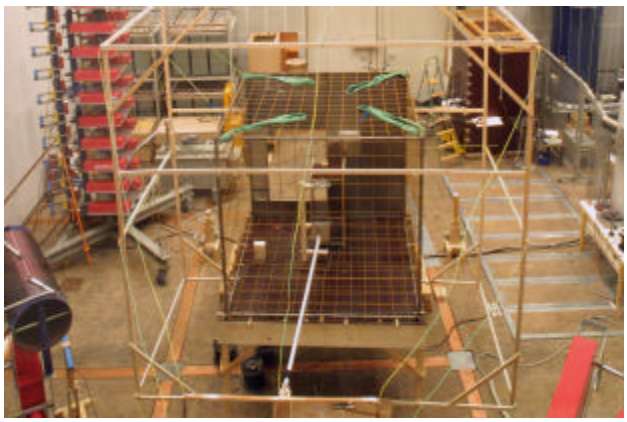

Fig. 2. Test setup in the laboratory

2.2 Test Generators and Currents

The Figures 1 and 2 show the test current injection into the roof via a 2 m long aluminum tube of 35 mm diameter. The current return paths from the floor termination steel plate are formed by an array of eight copper return conductors (10 mm^2 each) that are quasi-coaxially arranged around the steel cage at 1 m from the sides and at about 0,7 m from the current injection terminal.

The currents were injected at three different location into the roof of the outer cage, namely, to the center at (*x*, *y*, *z*) of (1, 1, 2), to the middle of a lateral edge at (1, 0, 2), and to the corner at (2, 0, 2).

Table 1 gives the parameters of the unidirectional test currents, where I_p is the current peak value, T_1 the front time and T_2 the decay time to half-value. Examples of the currents waveforms are shown in the Figures 3 - 5.

Table 1: Parameters of the test currents.

Simulated return stroke type	I_p (kA)	T_1 (µs)	T_2 (µs)
Positive	77	10	380
Negative first	- 16	1	55
Negative subsequent	- 4,8	0,25	12

Three impulse current generators were specially adapted to simulate the above-mentioned three currents [7,8]. The slow waveform currents were generated by an under-critically damped 100 kJ capacitor bank employing crowbar technique to get a unidirectional waveform. The microsecond waveform currents were obtained from an over-critically damped 100 kJ capacitor bank with an additional peaking circuit (low impedance peaking capacitor and an auxiliary peaking spark gap) to increase the current steepness. The sub-microsecond waveform generator consisted of a 216kV three-stage Marx generator with an erected capacitance of 400 nF also equipped with a peaking circuit.

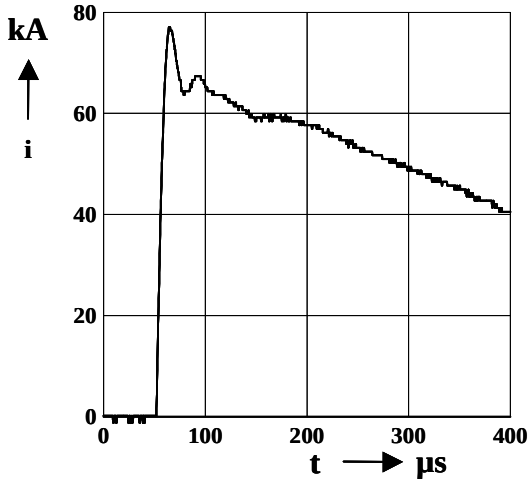

Fig. 3. Slow waveform (T_1 = 10 µs)

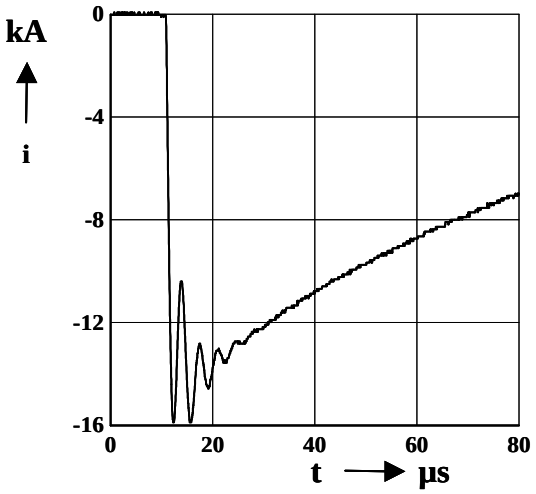

Fig. 4. Microsecond waveform (T_1 = 1 µs)

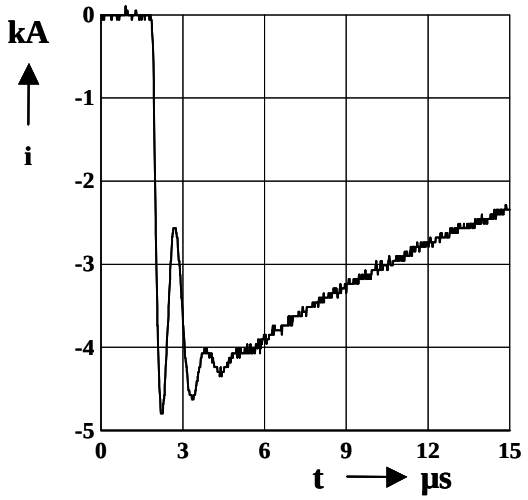

Fig. 5. Sub-microsecond waveform (T_1 = 0,25 µs)

2.3 Magnetic Field and Induced Voltage Measurement

The magnetic fields and their derivatives were determined at four distinct measuring locations inside the test structure, in the center, about midway between the center and the wall, close to the wall, and close to the corner. An overview of the individual *x, y,* and *z* coordinates are given in Table 2 for the single and double layer arrangements.

Table 2: Magnetic fields measurement locations.

	Test structure arrangement					
	Single layer (AI)			Double layer (AII, AIII)		
Location	*x* (m)	*y* (m)	*z* (m)	*x* (m)	*y* (m)	*z* (m)
Center	1	1	1	1	1	1
Midway	1	0,5	1	1	0,5	1
Close to wall	1	0,15	1	1	0,3	1
Close to corner	1,85	0,15	1	1,7	0,3	1

The magnetic field derivatives (dH/dt) were measured using shielded loop sensors of 15 cm and 20 cm diameter (Figure 6). The signals were transferred to the digital scopes (HP 54510A, 200 MHz single shot bandwidth) via 200 MHz fiber optic link systems NanoFast OP 300-2A. The magnetic fields were derived from the (dH/dt)-waveforms by numeric integration. Background noise originating from the current generator spark gaps (start gaps, crowbar gap, peaking circuit gaps) was eliminated during the integration process.

The induced open circuit loop voltage between roof and floor of the test structure was measured with a 0,5 mm^2 copper wire terminating into a 500 Ω probe. This signal, too, was transferred via fiber optic link.

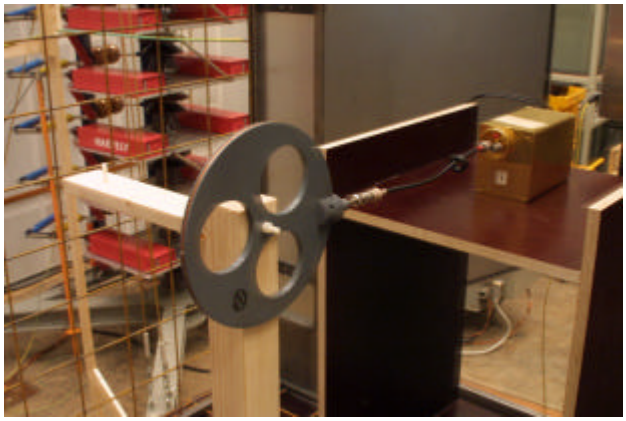

Fig. 6. dH/dt measurement

3. MEASURED WAVEFORMS

Following, example waveforms are given for the measured quantities magnetic field derivative (dH/dt), magnetic field (H), and voltage between roof and floor (u_l). Of course, there was some variation in the recorded waveforms. Therefore, the examples given are intended to identify the basic structure common to the majority of signals.

Figures 7 and 8 show a typical dH/dt- and the resulting H-waveform. This example is the measured *x*-component close to the wall for the microsecond waveform injected to the lateral edge of the roof. The dH/dt-waveform is basically proportional to the current derivative, but with some superimposed component: The zero crossing during the decay portion occurs not before about 50 µs ... 60 µs, which is about equal to the time to half-value of the injected current. As a consequence, the magnetic field rise is much slower compared to the injected current rise. Such an effect is also known for carbon fiber composite enclosures [5].

To characterize this effect, the 10% to 90% rise time T_a of the magnetic field is given in Table 3 for the different current waveforms and test structures. The values given are mean values over about 70% of all measured signals, excluding weak signals that could hardly be distinguished from the background noise. The results for the double-layer test structures, AII and AIII, are quite similar. Compared to the single-layer test structure AI, the magnetic field rise times for the double-layer test structures are significantly lower. This effect is more pronounced the faster the injected current rise.

Table 3: Mean magnetic field rise time T_a

Front Time T_1	Mean rise time T_a		
	AI	AII	AIII
10 µs	140 µs	210 µs	210 µs
1 µs	18 µs	28 µs	35 µs
0,25 µs	2,9 µs	6,0 µs	6,5 µs

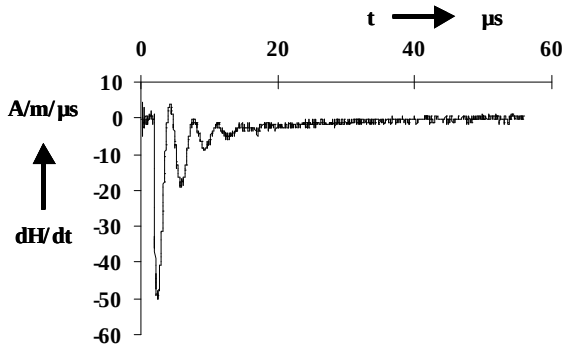

Fig. 7. Example of the magnetic field derivative (dH/dt)

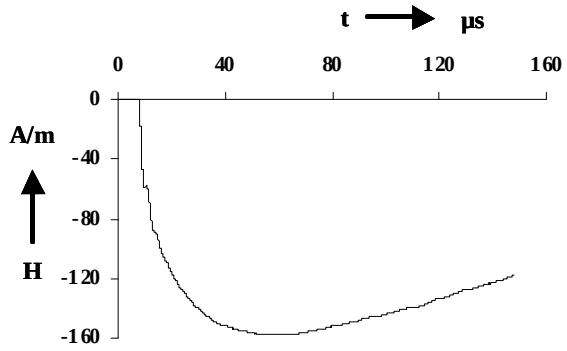

Fig. 8. Example of the magnetic field (H)

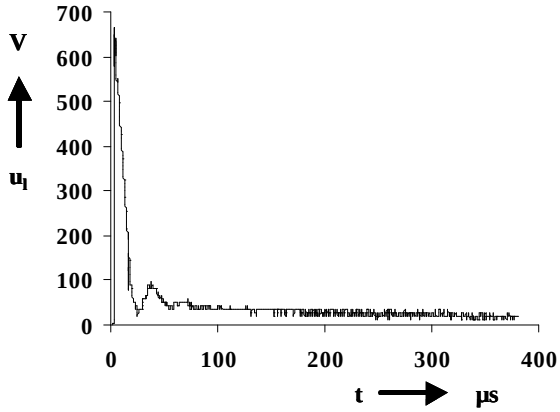

Fig. 9. Example of the induced roof-to-floor voltage

An example of the induced open circuit voltage between roof and floor of the test structure is reproduced in Figure 9 (single cage, center current injection, slow waveform). The voltage is composed of an inductive component, proportional to the current derivative di/dt, and of a resistive component proportional to the current i. During the current front the inductive component clearly dominates. The resistive component can be seen during the current decay, where the di/dt is low. With time, it becomes almost equal to the DC resistance of the test structure multiplied with the current. For the microsecond and sub-microsecond waveforms the resistive component almost disappears.

4. SHIELDING EFFECTIVENESS OF A SECOND REINFORCEMENT LAYER

For the determination of the additional shielding effectiveness of a second reinforcement layer it is distinguished between three groups of measured signals:

- Magnetic field derivative dH/dt which is mainly responsible for voltages induced into open circuit loops inside the structure.
- Magnetic field H which is mainly responsible for currents induced into short circuit loops inside the structure.
- Induced voltage between roof and floor which can be considered as an indicator for voltages appearing in large loops connected to roof and ground, like electrical lines leading to air conditioning equipment on the roof.

For the determination of the relative amplitudes of these quantities between the three types of test structures only 75% of the about 350 measured signals could be used. Some signals were too weak to distinguish from background noise. In a few other cases the polarity of the measured dH/dt-waveforms was opposite for the different test structures. In these cases the signals usually were low, too, hardly above background noise.

4.1 Magnetic Field Derivative

In order to characterize the additional shielding effectiveness of a second reinforcement layer for the magnetic field derivative, the ratios of the peak dH/dt are built, comparing the test structures AI/AII and AI/AIII. The results are given in Table 4 for the different injection current waveforms, injection points, and dH/dt-components (*x, y, z*). In this table only the usable components are listed.

Table 4: Ratios of the magnetic field derivatives

Front Time T_1	Injection point	Co-ordinate	dH/dt	
			AI/AII	AI/AIII
10 µs	Center	*z*	2,65	2,09
	Lateral Edge	*x*	2,49	2,81
		z	3,19	3,67
	Corner	*x*	2,29	2,60
		y	4,34	4,65
		z	2,50	2,55
	Mean		**2,9**	**3,1**
	Std. dev.		0,8	0,9
1 µs	Center	*z*	2,90	2,93
	Lateral Edge	*x*	3,30	3,27
		z	2,40	2,54
	Corner	*x*	3,25	3,18
		y	5,38	6,10
		z	3,13	2,80
	Mean		**3,4**	**3,5**
	Std. dev.		1,0	1,3
0,25 µs	Center	*x*	-	5,63
	Lateral Edge	*x*	3,24	4,59
		z	2,73	3,34
	Corner	*x*	3,65	4,18
		y	3,20	6,89
		z	3,57	4,92
	Mean		**3,3**	**4,9**
	Std. dev.		0,4	1,2

With exception of the sub-microsecond waveform the ratios are quite similar for AI/AII and AI/AIII. There is a tendency towards better shielding for faster rising current waveforms. This indicates that the coupling mechanism is dominated by the magnetic fields resulting from the current flow through the reinforcement grid and not by field penetration through the grid apertures. The faster the current rise, the more the current is displaced to the outer grid of the double-layer test structures. In conclusion, the shielding for the magnetic field derivative is improved roughly by a factor of 3 to 4 (or 9 dB to 12 dB) for the different current waveforms.

4.2 Magnetic Field

Similar to the procedure given in section 4.1, the additional shielding effectiveness is determined for the ratios of the peak magnetic fields. Due to the limited space, Table 5 summarizes the resulting mean values and standard deviations (Std. dev.) without presenting the individual data.

The overall tendency is similar to the results obtained for the magnetic field derivative, with a trend towards better shielding against the fields of faster rising currents. The improvement of the shielding for the magnetic field, however, is lower by a factor of about 2 compared to that obtained for the magnetic field derivative. For the different waveforms, the improvement is between 1,4 and 2,2 (or 3 dB and 7 dB).

Table 5: Ratios of the magnetic fields

Front Time T_1		H	
		AI/AII	AI/AIII
10 µs	**Mean**	**1,4**	**1,4**
	Std. dev	0,3	0,5
1 µs	**Mean**	**1,9**	**1,7**
	Std. dev	0,3	0,4
0,25 µs	**Mean**	**2,2**	**2,2**
	Std. dev	0,2	0,7

4.3 Induced Roof-to-Floor Voltage

For the voltages induced between the roof and the floor of the test structures, mean values can only be presented for the comparison of the test structures AI and AIII. For the test structure AII the measured data are not conclusive. For a given injection current waveform, the ratios (AI/AII) significantly depend on the injection point: The roofs of the outer and the inner grid of test structure AII are only connected at the four corners. In case of the center injection point, there is almost no current flow along the roof of the inner cage, which forms a part of the induction loop. This is quite different in case of the corner injection, where remarkable parts of the current flow through the inner cage roof.

In case of the test structure AIII with multiple bonding of the inner and outer grids, the ratios (AI/AIII) are not much dependent on the current injection point. The ratios (AI/AIII) for the induced roof-to-floor voltage are 4,4, 4,3, and 6,2 for the slow, microsecond and sub-microsecond waveform, respectively. This equals to a range of 13 dB to 16 dB.

5. CONCLUSIONS

The improvement in the shielding of a double-layer reinforced concrete compared to a single-layer one during a direct strike was determined experimentally for a variety of anticipated lightning currents. It was found that the magnetic fields inside a reinforced structure have a significantly slower rise than the injected current. This effect is even more pronounced for a double-layer structure. For the faster rising injection currents, the improvement of the shielding is better, due to the increased current displacement towards the outer reinforcement grid. The shielding improvement ranges from 9 dB to 12 dB for the magnetic field derivatives, and from 3 dB to 7 dB for the magnetic fields.

6. REFERENCES

[1] IEC 61312-1 (1995-03): *Protection against lightning electromagnetic impulse - Part 1: General principles*

[2] IEC/TS 61312-2 (1999-08*): Protection against lightning electromagnetic impulse (LEMP) - Part 2: Shielding of structures, bonding inside structures and earthing*

[3] König M., "Transient overvoltages in large buildings with natural components during a direct strike", *23rd Int. Conf. on Lightning Protection (ICLP),* Firenze (I), 1996, pp. 545-550

[4] König M., Steinbigler H., "Magnetic field distribution inside a gridlike spatial shield in case of a direct lightning strike", *24th Int. Conf. on Lightning Protection (ICLP)*, Birmingham (UK), 1998, pp. 264-269

[5] D'Amore M., Sarto M.S., "Time-domain analysis of the lightning induced effects on wire networks inside carbon fiber composite enclosures", *25th Int. Conf. on Lightning Protection*, Rhodes, (GR), 2000, pp. 284-289

[6] Schnetzer G.H., Fisher R.J., "Measured responses of a munitions storage bunker to rocket-triggered lightning", *21st Int. Conf. on Lightning Protection (ICLP)*, Berlin (DE), 1992, pp. 237-242

[7] Zischank W.J., Heidler F. Wiesinger J., Kern A., Seevers M., "Shielding effectiveness of reinforced concrete cable ducts carrying partial lightning currents", *24th Int. Conf. on Lightning Protection (ICLP)*, Birmingham (UK), 1998, pp. 735-740

[8] Wiesinger J., Zischank W.J, *"Chapter 2: Lightning Protection"* in: Volland H.: *"Handbook of Atmospheric Electrodynamics"*, Volume II. CRC Press, Boca Raton, London, Tokyo, 1995

Address of Main Author:
Dr.-Ing. Wolfgang Zischank
Universität der Bundeswehr München
Fakultät für Elektrotechnik, EIT7
Werner-Heisenberg-Weg 39
D - 85 579 Neubiberg
Germany